1-17-2007

Modeling of Intermediate Phase Growth

Alexander Umantsev

Fayetteville State University, aumantsev@uncfsu.edu

Modeling of intermediate phase growth

A. Umantsev[a)]

Department of Natural Sciences, Fayetteville State University, 1200 Murchison Road, Fayetteville, North Carolina 28301

We introduced a continuum method for modeling of intermediate phase growth and numerically simulated three common experimental situations relevant to the physical metallurgy of soldering: growth of intermetallic compound layer from an unlimited amount of liquid and solid solders and growth of the compound from limited amounts of liquid solder. We found qualitative agreements with the experimental regimes of growth in all cases. For instance, the layer expands in both directions with respect to the base line when it grows from solid solder, and grows into the copper phase when the solder is molten. The quantitative agreement with the sharp-interface approximation was also achieved in these cases. In the cases of limited amounts of liquid solder we found the point of turnaround when the compound/solder boundary changed the direction of its motion. Although such behavior had been previously observed experimentally, the simulations revealed important information: the turnaround occurs approximately at the time of complete saturation of solder with copper. This result allows us to conclude that coarsening of the intermetallic compound structure starts only after the solder is practically saturated with copper. © *2007 American Institute of Physics*. [DOI: 10.1063/1.2424530]

I. BACKGROUND

A. Experiment

Physical metallurgy of soldering presents many interesting problems: transformations in the solder, transformations in the contacts, and mechanical and electrical properties of the joints.[1] One of the problems that is critical for soldering industry is the formation and growth of an intermediate phase between the solder and the contact. The occurrence of an intermediate phase near 50 at. % of Sn in the Cu–Sn system at temperatures below 415 °C was observed in 1904.[2] This transformation was found to be associated with significant amount of heat of formation (first-kind transition), but details regarding the nature of the phase mostly have been unknown at the time. Later on this phase (η phase) was identified as an intermetallic compound (IMC) Cu_6Sn_5.[3] The compound Cu_6Sn_5 undergoes another phase transformation at approximately 189 °C, which was identified as a second-kind order-disorder transition ($\eta \leftrightarrow \eta'$) associated with the formation of a long-period superlattice.

The compound grows in the form of a layer with morphology strongly dependent on the temperature of soldering: Onishi and Fujibuchi[4] showed that the growth of IMCs from solid-state Cu–Sn diffusion couples results in a relatively planar layer of IMC. However, observations of the intermetallic growth in the solid-Cu(Ni)/liquid-Sn system (above the melting point of the solder) instead of a smooth layer always show rough, strongly undulated compound layers with scallops of the intermetallic phase.[5–7] With time scallops grow larger but fewer, indicating that the coarsening process takes place.[6,7] The problem of IMC layer growth has many challenges, the reasons for roughness and coarsening, to name

only a few. To describe this process Kim *et al.*[6,8] suggested a two-flux nonconservative Ostwald ripening model based on the assumption of rapid dissolution of Cu into the liquid solder. Hayashi *et al.*[5] suggested the fast dissolution of Cu_6Sn_5 along the grain boundary as the reason for scallop-edge appearance. However, the suggestion of the predominant dissolution in the system remained unsubstantiated. Boettinger *et al.*[9] studied the effect of thickness of Sn–Pb eutectic solders on IMC growth and dissolution of copper. The authors found that the dynamics of IMC/solder boundary was nonmonotonic: the boundary moved in the direction of the substrate for some time that depended on the thickness of the solder before turning in the direction of the solder.

To resolve the problem of the mechanism of IMC layer formation and growth, Lord and Umantsev[10] conducted an experiment with the intent to capture the growth on the very early stages. Fast dipping and pulling of a copper coupon in liquid solder allowed the workers to study motion of the boundaries of the layer relative to the original solder/contact interface, the base line. On the basis of the experimental results the authors concluded that the growth of IMC layer from molten pure-Sn solder proceeds by the creation-dissolution mechanism (CDM): the leading edge of the IMC moves into the substrate and creates the compound, while the trailing edge, moving in the same direction but slightly slower, dissolves the newly formed compound. The small difference in the leading and trailing edge velocities entails the rate of growth of the IMC layer. Lord and Umantsev identified the dissolution of the grain boundaries as the primary reason for the formation of undulations of the IMC layer in the form of scallops and confirmed the suggestion made in Ref. 5. Quantitative analysis of the growth rates of a continuous IMC layer showed that the early stages are controlled by the kinetics of dissolution of the copper, with the kinetic coefficient of dissolution of copper in pure tin being

---

[a)]Electronic mail: aumantsev@uncfsu.edu

101, 024910-1

~1 mm/s mfr. On the basis of this analysis and other litera-
ture Lord and Umanstev introduced a hypothesis that coars-
ening of IMC layer starts around the time of saturation of the
solder.

B. Theory

For better understanding of physical metallurgy of inter-
mediate phase formation and growth one needs a theoretical
or computational model capable of describing all different
regimes of this process. A number of authors tried to address
the problem of intermediate phase growth in the framework
of a multiphase Stefan problem.[11–13] Gibbs derived a system
of two equations for the growth-rate constants and studied
different limiting forms of the solution.[12] Although this ap-
proach proved not to describe soldering correctly (e.g., the
thickness of IMC layer growing from the molten solder does
not obey square-root time law[7] which follows from the
theory), it still captures essential physics of the intermediate
phase growth, for instance, different regimes of growth de-
pending on different ratios of diffusion coefficients in solder,
IMC, and copper phases. That is why we extended this
method on a particular case that describes liquid-state solder-
ing and presented the results in Appendix A.

C. Computation

Many problems of soldering may be resolved with the
help of the numerical simulations. Although significant
progress in the problem of solder microstructure formation
and evolution has been made in the past few years,[19] the
problem of modeling of IMC growth remains unresolved. A
numerical model capable of reproducing experimental results
on the IMC layer formation and growth is a multifaceted
project with many separate components that affect the out-
come of the transformation. For instance, nucleation of the
intermediate phase or growth of grains, which make up the
layer of IMC, should be included in the dynamical scheme
describing the evolution of the system. However, in the
present publication we disregard the grain structure of the
IMC layer and consider only the one-dimensional evolution
of it from a solid/solid or solid/liquid diffusion couple. Simu-
lation of the full, two—or three-dimensional, structure and
evolution of the growing IMC layer will be addressed in a
following publication. Wherever possible the numerical re-
sults will be compared to the theoretical and experimental
ones. Such models may help in the analysis of many of the
experiments on crystallization, which may be described as
the growth of a layer of intermediate phase between a molten
phase of one composition and solid phase of another compo-
sition (e.g., growth of superconducting layers of MgB_2 or
aluminizing treatment of the surface of nickel-base superal-
loys).

II. CONTINUUM METHOD

A. The free energy of the system

Continuum method has become the method of choice for
modeling of very different phase transformations in the past
decade. The success of the method is due to its computa-

tional flexibility and ability to transcend the constraints of
limited spatial/temporal scales, imposed by strictly micro-
scopic or macroscopic methods, hence becoming a truly mul-
tiscale one. Phase transitions in materials may be character-
ized by one or more coarse-grained continuous variables η_l
commonly called order parameters (OPs), which take on
specified values in the phases of interest, and the densities of
different components, ρ_1, ρ_2, ρ_3,…, which specify the over-
all composition of an alloy. The free energy in the continuum
approximation becomes a functional over the entire system
with the free energy density being a function of these vari-
ables as well as their gradients. Details of the method may be
found in the literature.[14–17]

We define the process of intermediate phase growth as
simultaneous crystallization plus ordering of a growing
phase. Thus, the thermodynamic system of interest here
should be able to undergo liquid$\leftrightarrow$solid and order$\leftrightarrow$disorder
transitions, which may be accompanied by solute redistribu-
tion. Crystallographic analysis shows that the transition from
disordered solid solution (fcc-copper phase) to ordered inter-
metallic compound (η phase) is of the first kind, while the
$\eta\leftrightarrow\eta'$ transition at lower temperatures is of the second
kind.[3] The latter does not play a significant role in soldering
with molten solders and will not be considered in the present
work; neither will ε phase (Cu_3Sn) be considered. However,
we would like to notice that extension of the model on $\eta\leftrightarrow\varepsilon$
and $\eta\leftrightarrow\eta'$ transitions is straightforward. In the present pub-
lication we consider the case of a binary system, so that the
compositions of both phases may be described by the mole
fraction of the solute, c, instead of the densities of the com-
ponents. Hence, the phase space of the system will include
three coordinates: two OPs representing crystallization, ξ,
and ordering η and c representing the concentration of solute
(Cu in the present treatment).

In the following we use the Gibbs free energy in the
so-called square-gradient approximation:

$$F = \int \left[f(c,\xi,\eta) + \frac{1}{2}\kappa_\xi(\nabla\xi)^2 + \frac{1}{2}\kappa_\eta(\nabla\eta)^2 \right] d^3x, \quad (1)$$

with the following expression for the free energy density:

$$f(c,\xi,\eta) = f_s(c) + (1/2)a_\xi\omega^2(\xi) + [f_c(c) - f_s(c)]\nu(\xi)$$
$$+ (1/2)a_\eta\omega^2(\eta) + [f_i(c) - f_c(c)]\nu(\eta),$$

$$\omega(x) = x(1-x),$$

$$\nu(x) = x^2(3-2x). \quad (2)$$

The thermodynamic parameters, barrier heights a_q, and gra-
dient energy coefficients κ_q, $q=\xi$, and η, are associated with
the interfacial properties. For the details of the choice of the
free energy density consult Ref. 17.

As one can see from Eq. (2), the free energy of this type
does not present direct interactions between crystallization
and ordering processes expressed by cross terms of the type
$\xi^y\eta^z$. In a thermodynamic system described by the free en-
ergy, Eq. (2), interactions between the processes of crystalli-
zation and ordering proceed indirectly through the concen-
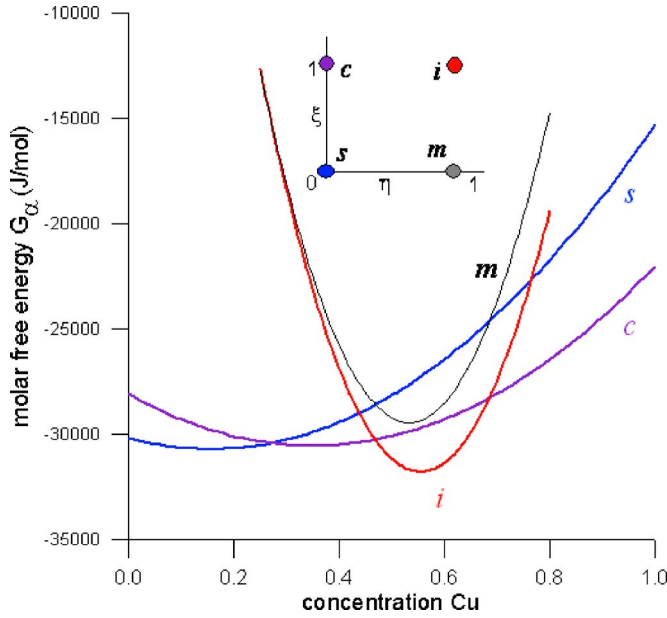tration field. In the OP plane (ξ,η) of the phase space there

FIG. 1. (Color online) Molar free energies of different phases in the system obtained from Thermocalc® database: (*s*:) atomic-liquid solution; (*c*) fcc-solid solution; (*i*) intermetallic compound; (*m*) molecular liquid. Insert: The order-parameter plane of the phase space of the system.

TABLE I. Bulk-phase material parameters at $T = 275\ °C$.

Properties	Phase		
	Copper (*c*)	IMC Cu$_6$Sn$_5$ (*i*)	Solder (*s*)
$G_{\alpha,0}$ (J/mol)	-2.8086×10^4	3.1717×10^4	-3.0181×10^4
$G_{\alpha,1}$ (J/mol mfr)	-1.4111×10^4	-2.2886×10^5	-6.7742×10^3
$G_{\alpha,2}$ (J/mol mfr^2)	4.0346×10^4	4.1234×10^5	4.3339×10^4
Molar volume v_α^m (m^3/mol)	7.12×10^{-6}	117.87×10^{-6}	16.3×10^{-6}
$f_{\alpha,2}$ (J/m^3 mfr^2)	0.567×10^{10}	0.350×10^{10}	0.266×10^{10}
Equilibrium concentrations	0.976 50	0.616 35	
		0.545 11	0.061 988
$C_{\alpha/\beta}$ and $C_{\beta/\alpha}$ (mfr)	0.369 64		0.174 82
Diffusion coefficients D_α (m^2/s)	1.04×10^{-16}	5.2×10^{-16}	5.2×10^{-13} (liquid)
Diffusion coefficients D_α (m^2/s) ($T = 220\ °C$)	1.04×10^{-16}	5.2×10^{-16}	5.2×10^{-15} (solid)

are four points that correspond to equilibrium phases: (*s*: ξ $=0$, $\eta=0$) atomic-liquid solder phase, (*c*: $\xi=1$, $\eta=0$) fcc-solid copper phase, and (*i*: $\xi=1$, $\eta=1$) intermediate phase. The fourth equilibrium point (*m*: $\xi=0$, $\eta=1$) may be interpreted as a molecular liquid phase with the free energy

$$f_m(c) = f_s(c) + f_i(c) - f_c(c). \qquad (3)$$

The free energies of the liquid solution, $f_s(c)$, fcc-solid solution, $f_c(c)$, and intermediate η phase, $f_i(c)$, may be obtained either from first-principles calculations or from an appropriate database. In this paper the molar free energies of the phases $G_\alpha(c)$, $\alpha=c, i, s$, at $T=275\ °C$ were obtained from Thermocalc® database.[18] They are depicted in Fig. 1 together with the phase *m* calculated using Eq. (3); insert in Fig. 1 shows the OP plane of the phase space (c, ξ, η). For the numerical calculations the molar free energies of the phases were converted into the free energy densities by dividing them by the respective molar volumes v_α^m.

In the present publication the free energies of phases were taken in the parabolic approximation

$$f_\alpha(c) = f_{\alpha,0} + f_{\alpha,1}c + \frac{1}{2}f_{\alpha,2}c^2, \qquad (4)$$

because it greatly simplifies the common-tangent construction for the determination of the equilibrium phase compositions (details are given in Appendix B). The free energy coefficients, the molar volumes, and the two-phase equilibrium concentrations are given in Table I. Here and below $C_{\alpha/\beta}$ means concentration of α phase in equilibrium with β phase and $\beta=c, i, s$.

B. Dynamics of order parameters and diffusion of species

If the system is set up in nonequilibrium state, it will be evolving in the direction of equilibrium due to the presence of the thermodynamic driving force, which is expressed as the variational derivative of the free energy. As OPs do not obey any conservation constrains, their evolution equations are of relaxational type and are known as the time-dependent Ginzburg-Landau equations (TDGLEs),

$$\frac{d\xi}{dt} = -\gamma_\xi \left(\frac{\delta F}{\delta \xi} \right)_{T,P}, \qquad (5)$$

$$\frac{d\eta}{dt} = -\gamma_\eta \left(\frac{\delta F}{\delta \eta} \right)_{T,P}. \qquad (6)$$

Here the response coefficients γ_q set the relaxation time scales $\tau_q = (\gamma_q a_q)^{-1}$.

As we pointed out above, the diffusional transformations are characterized by another set of variables, densities ρ_i, which also may undergo changes together with the order parameters. The fundamental difference between the former and the latter is in the conservation constraints that the densities must obey. This difference is translated into the different type of evolution equation, that is, diffusion equation for the mole fraction of solute,

$$\frac{dc}{dt} = \nabla \left[M(c, \xi, \eta) \cdot \nabla \frac{\delta F}{\delta c} \right], \qquad (7)$$

where M is the solute mobility coefficient. The system of coupling diffusion-type equations, Eqs. (5)–(7), describes the dynamics of the system. The temperature of the system will be assumed as constant.

To account for unequal diffusivities in the liquid, solid, and intermediate phases, which is critical for the present treatment, the solute mobility coefficient M must be assumed to be OP dependent. For a discussion of choices of such relationships one may consult Ref. 14. In the present study we are using the following function:

$$M(c, \xi, \eta) = M_s + (M_c - M_s)\xi + (M_i - M_c)\eta. \quad (8)$$

The mobilities of the solder, M_s, copper, M_c, and intermediate phase, M_i, can be easily recovered if the diffusion coefficients in these phases are known, because

$$D_\alpha = M_\alpha f_{\alpha,2}. \quad (9)$$

Notice that in the present treatment for the mobilities to be concentration independent we do not need to introduce the "thermodynamic factor" $c(1-c)$ because the free energies of phases are taken in the quadratic approximation, Eq. (4). The diffusion coefficients used in the present work are given in Table I.

C. Interfacial material parameters

The parameters, a_q, κ_q, and γ_q, are associated with equilibrium and dynamic properties of the interfaces and should be identified from experimentally measurable interfacial quantities. In case of phase transitions in pure materials these parameters may be obtained from physical or numerical experiments that bring the values of the interfacial energy σ_q, interfacial thickness δ_q, and kinetic coefficient $k_{q,T}$. Recently[17] the author considered a problem of extracting these parameters from physical or numerical experiments in binary or multicomponent alloy systems. He showed that in the case of a linear system, that is, if $f_{\alpha,2} \approx f_{\beta,2} \equiv f_2$, the barrier-height parameter a_q, gradient energy κ_q, and relaxation coefficient γ_q may be expressed as follows:

$$a_q = 24\frac{\sigma_q}{\delta_q} - 4f_2(C_{\beta/\alpha} - C_{\alpha/\beta})^2,$$

$$\kappa_q = \frac{3}{2}\sigma_q\delta_q,$$

$$\gamma_q = \frac{k_{q,C}}{6\delta_q f_2(C_{\beta/\alpha} - C_{\alpha/\beta})}. \quad (10)$$

Here $k_{q,C}$ is the solute kinetic coefficient taken from the relation $V = k_{q,C}(C_{\alpha/\beta} - c_\alpha)$, where c_α is the actual concentration in the α phase in front of the interface. As one can see from Eqs. (10), in order to obtain the interfacial parameters $(a_q, \kappa_q, \gamma_q)$ of alloys, one still needs the values of the same interfacial properties $(\sigma_q, \delta_q, k_{q,C})$.

Ravelo and Baskes[20] conducted a numerical experiment and calculated the reversible work required to pull pure solid copper from pure liquid tin. From this experiment the authors got relatively high values of 0.76–0.89 J/m² for the tin-copper solid/liquid interfacial energy at $300\,\text{K} < T < 1100\,\text{K}$. We believe that such high values of the interfacial energy appear because alloying was not allowed in the simulations. Lord and Umantsev studied early stages of soldering reactions and showed that the experimental data on kinetics of dissolution of copper in tin can be interpreted through a relationship for the interfacial velocity $V = k_{\xi,C}(C_{s/i} - c_s)$. For the compositional kinetic coefficient they found the value of $k_{\xi,C} \approx 1$ mm/s mfr in the temperature range of $520\,\text{K} < T < 620\,\text{K}$. Because the experiments were done on the early stages of the soldering reaction when the IMC layer is very

thin and thus may be ignored, the obtained value of the compositional kinetic coefficient can be attributed to the two-phase solid/liquid Cu–Sn system. As this system satisfies the conditions of linearity, see Table I, the interfacial parameters $(a_\xi, \kappa_\xi, \gamma_\xi)$ can be calculated using Eqs. (10); the interfacial thickness δ_ξ was assumed to be equal to 1 nm. The parameters $(a_\eta, \kappa_\eta, \gamma_\eta)$ may be obtained from the first-principles calculations or from experimental data on order↔disorder transition in solid state. Because such data were not available these parameters were estimated here as $a_\eta = (1/2)a_\xi$, $\kappa_\eta = (1/2)\kappa_\xi$, and $\gamma_\eta = \gamma_\xi$. The calculated material parameters used for computations are given in Table II.

TABLE II. Interfacial material parameters.

Parameter	Transformation	
	Crystallization (ξ)	Ordering (η)
Barrier height α_q (J/m³)	1.86×10^{10}	0.93×10^{10}
Gradient energy coefficient κ_q (J/m)	1.2×10^{-9}	0.60×10^{-9}
Relaxation coefficient γ_q (m³/J s) ($T = 275\,°\text{C}$)	2.2×10^{-4}	2.2×10^{-4}
Relaxation coefficient γ_q (m³/J s) ($T = 220\,°\text{C}$)	2.2×10^{-6}	2.2×10^{-6}

D. Scaling

As it has been proven many times, numerical calculations may be done more efficiently, and the results are easier to interpret if the calculations are performed in scaled units, with the scales chosen to reflect the physical properties of the system under consideration. In the present treatment we choose the following scales:

$$\text{energy density unit} = a_\xi = 1.86 \times 10^{10} \text{ j/m}^3,$$

$$\text{space unit} = \sqrt{\frac{\kappa_\xi}{a_\xi}} = 0.25 \text{ nm},$$

$$\text{time unit} = \frac{1}{\gamma_\xi a_\xi} = 0.25 \text{ }\mu\text{s}. \quad (11)$$

All the numerical results presented in the next section are in the scaled units of length and time. Scaling of the diffusion equation, Eq. (7), yields the dimensionless diffusion coefficients in the bulk phases,

$$R_s = \frac{D_s}{\gamma_\xi \kappa_\xi} \approx 2, \quad R_i = \frac{D_i}{\gamma_\xi \kappa_\xi} \approx 2 \times 10^{-3}, \quad (12)$$

$$R_c = \frac{D_c}{\gamma_\xi \kappa_\xi} \approx 4 \times 10^{-4}.$$

Only one-dimensional numerical simulations are presented in this publication. The straightforward explicit numerical technique was used to solve the dynamical equation; no antitrapping currents were used.

III. NUMERICAL RESULTS

The numerical simulations described in this paper correspond to soldering in a Cu–Sn couple with different amounts of solder (tin) when the copper part of the couple is placed on an inert substrate (e.g., computer board). In the soldering industry two significantly different situations are usually encountered: "solid-state" soldering and "liquid-state" soldering. Experimentally the solid-state soldering is more difficult to realize due to necessity to establish a completely uniform contact between the components of the couple. The latter may be achieved by one of the following techniques: electrodeposition of tin, pretinning of copper, or polishing of solid parts of the couple and clamping them together. The technical details of experiments are not important for the physical metallurgy of the intermediate phase formation and are not reflected in the simulations presented here. The main difference between the two situations is the temperature of the process, which translates into differences of many physical parameters: physical state and viscosity of the solder, free energies of the phases, interfacial parameters, etc. However, by far the greatest effect of the temperature difference is on the diffusion properties of the solder. Pertaining to the experimental situations the temperatures that we are reproducing are $T = 220\ °C$ for the solid-state soldering and $T = 275\ °C$ for the liquid-state one. Otherwise the simulations are completely isothermal and do not address the problem of the temperature effect in soldering, which should be a subject of a separate study.

In the present work the diffusion coefficient in the solder and both relaxation coefficients were chosen as the parameters that distinguish between solid-state and liquid-state solderings, see Tables I and II. In order to compare with physical experiments, three different cases were numerically computed: case A: IMC growth from an unlimited amount of solder with relatively low diffusion coefficient, case B: IMC growth from an unlimited amount of solder with relatively high diffusion coefficient, and case C: IMC growth from a limited amount of liquid solder with relatively high diffusion coefficient $(T = 275\ °C)$. These cases correspond respectively, to the experiments of Onishi and Fujibuchi on solid-state soldering (case A), of Lord and Umantsev on liquid-state soldering with unlimited amount of solder (case B), and of Boettinger *et al.* on liquid-state soldering with limited amount of solder (case C). Along with experiments, the results of numerical simulations with unlimited amounts of solder (cases A and B) will be compared with the theoretical results of the three-phase Stefan problem described in Appendix A.

Temporal behavior of the system was analyzed by calculating the positions of the interfaces of the IMC layer. The position of the IMC/solder interface with respect to the substrate, x_{is}, was determined as the numerical integral over the crystallization OP ξ, which measures the total amount of the solid phase (copper phase plus IMC). The total amount of the IMC phase, $\Delta X = x_{is} - x_{ci}$, was determined as the numerical integral over the ordering OP η. The difference between the two integrals yields the position of the IMC/copper interface with respect to the substrate, x_{ci}. For comparison of the nu-

merical results with the theory, positions of the interfaces were reckoned with that of the base line, x_b, and represented in the form

$$X_{\alpha i} \equiv x_{\alpha i} - x_b = A_\alpha t^{n_\alpha}, \tag{13}$$

while the theoretical results from Appendix A were scaled and represented in the forms

$$X_{\alpha i} = B_\alpha t^{1/2}, \quad B_\alpha = 2\beta_\alpha \sqrt{R_i}. \tag{14}$$

Comparison was made for n_α with $1/2$ and A_α with B_α.

We started with a layer of pure copper, approximately 200 space units thick, "sitting" on the inert substrate and a layer of pure tin solder of given thickness on top of the copper. Unlimited amount of solder was modeled by the thickness of the solder layer greater than the thickness of the diffusion layer at all times of simulation; when the concentration of Cu on the far end of the solder reached the level of 10^{-6}, the simulation was terminated. To avoid modeling precipitation of IMC phase, we started with a thin layer of the compound between significant amounts of pure tin and pure copper. In order to overcome the collapse of the initial layer of IMC, its thickness, $\Delta X \approx 20$ units, was slightly greater than the sum of the thicknesses of interfaces of this layer with the bulk phases (for the numerical parameters used in the present work the thicknesses of interfaces were approximately seven space units each). Position of the baseline, x_b, was determined as the average of x_{is} and x_{ci} at the beginning of simulations. Because the precipitation was replaced with the introduction of the initial layer, the system goes through the adjustment process first. Adjustment of the interfaces is very fast, 10–50 time units, while adjustment of the diffusion field is significantly slower, but was never more that 5% of the total simulation time. Adjustment periods were included into the time counts for comparison with the theory.
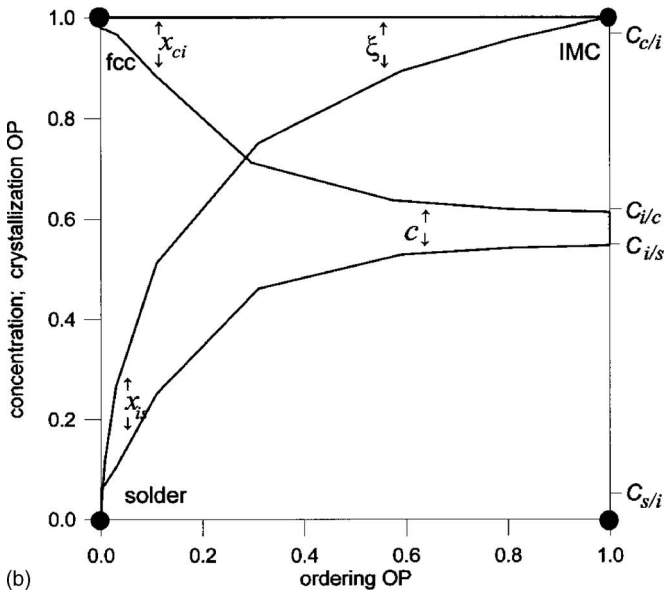
A. Case A: Solid-state soldering with unlimited amount of solder

In Fig. 2 concentration c, crystallization ξ, and ordering η OP fields are represented at the time $t = 2.0 \times 10^5$. Figure 2(a) shows the distributions of these fields in real space in the direction perpendicular to the interface. The boundaries of the IMC layer, x_{is} and x_{ci}, move in opposite directions with respect to the base line, which corresponds to the experiments of Onishi and Fujibuchi. In Fig. 2(b) the same fields are depicted in the phase space: crystallization OP ξ and concentration c as functions of the ordering OP η. Figure 2(b) shows that concentrations in the bulk phases adjacent to the interfaces closely approach their equilibrium values.

In Fig. 3 are depicted positions of the IMC/solder, x_{is}, and IMC/copper, x_{ci}, interfaces versus time. In the spirit of Eq. (13) the numerical data on the thickness of the IMC layer were fitted into the following relation: $\Delta X = A_{cs} \times t^{n_{cs}}$. The fitting produced $n_{cs} = 0.43 \pm 0.005$ and $A_{cs} = 0.61 \pm 0.01$. The numerical prefactor A_{cs} may be compared with the theoretical one, $B_{cs} = 0.67$, obtained from Eq. (A3) using the values of equilibrium solubilities from Table I. Proximity of the numerical exponent n_{cs} to $1/2$ and prefactor A_{cs} to B_{cs} allows us to consider the bulk diffusion as the rate limiting process
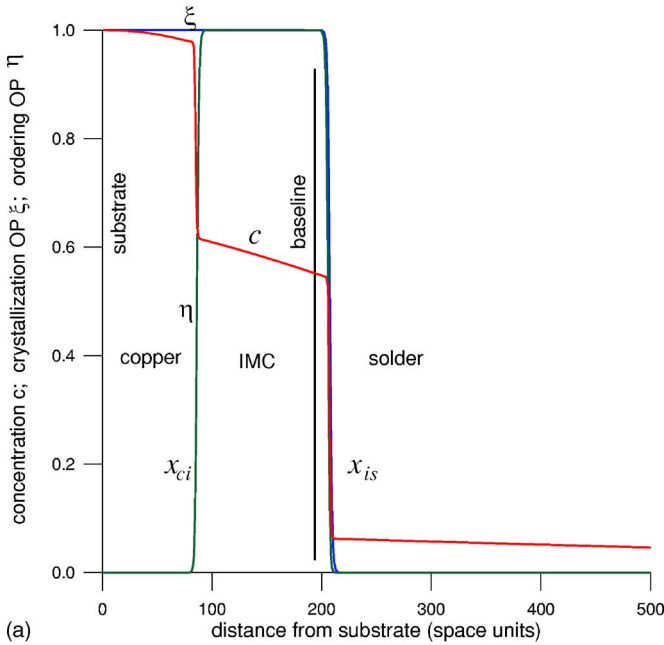
FIG. 2. (Color online) Case A: Distribution of concentration c, crystallization ξ, and ordering η OP fields at $t = 2 \times 10^5$. x_{is} and x_{ci} are positions of the boundaries. (a) Spatial distribution of the fields perpendicular to the interface. (b) Distributions of the fields in the phase space.

in solid-state numerical simulations. The quantitative correlation between the theory and experiment has been verified in Ref. 13.

B. Case B: Liquid-state soldering with unlimited amount of solder

In liquid-state simulations the system goes through a substantial self-adjustment process, which ends up with the formation of a "nucleus" in the form of a thin partially ordered layer of solid IMC of composition close to the equilibrium. With time the IMC layer orders and moves in the direction of the copper, which means that the molten solder dissolves the copper phase. In Fig. 4 are depicted spatial distributions of the ordering OP η and concentration c for the
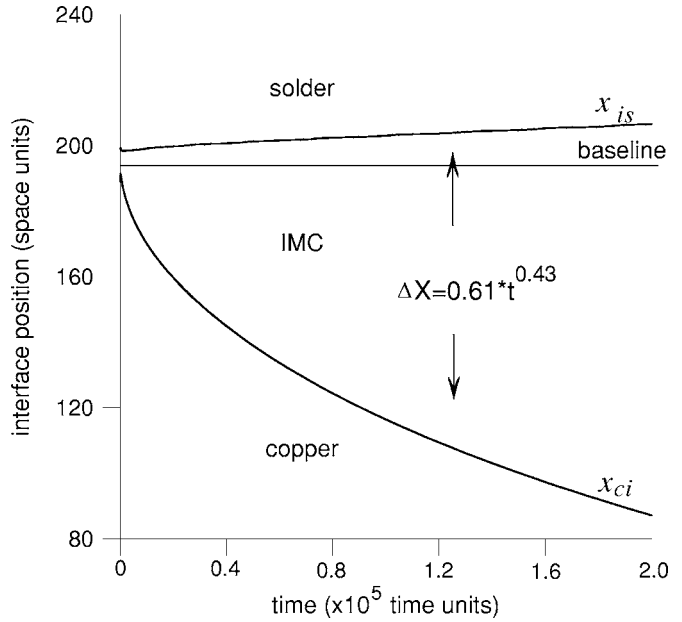

FIG. 3. Case A: Positions of the IMC/solder and IMC/copper boundaries vs time.

nucleus after 10^5 time units, and the layer after a significant soldering time of 12×10^5 (the distributions of crystallization OP ξ is not shown).

In Fig. 5 are depicted positions of the IMC/solder, x_{is}, and IMC/copper, x_{ci}, interfaces versus time. Comparison with the theory and experiments was carried out with respect to the average position of the layer relative to the base line, $X_i = (1/2)(X_{ci} + X_{is})$, and the thickening of the IMC layer, ΔX. Thickening of IMC fitted the power law with $n_{cs} = 0.19$ and $A_{cs} = 0.95$ and did not obey the parabolic law due to strong interactions between the interfaces through the layer. This result may be compared with experiments of Gagliano and
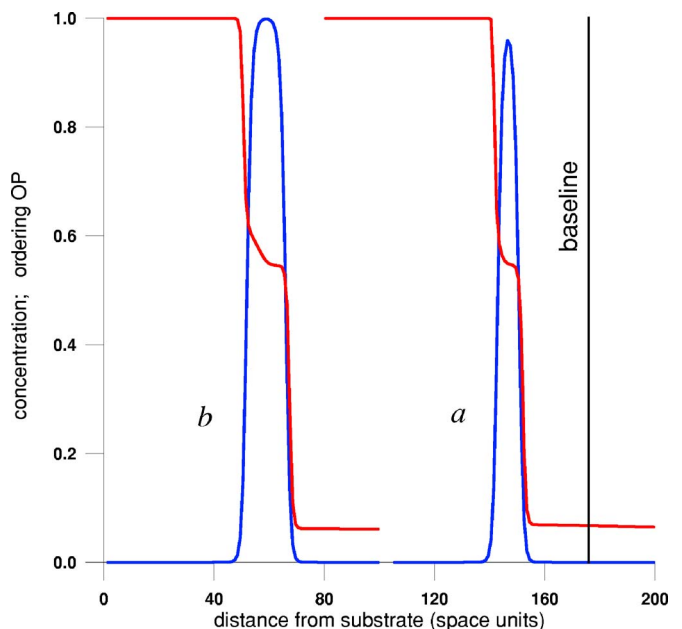

FIG. 4. (Color online) Case B: Spatial distributions of the ordering OP η and concentration c fields. (a) Nucleus of IMC at $t = 10^5$; (b) layer of IMC after $t = 12 \times 10^5$.
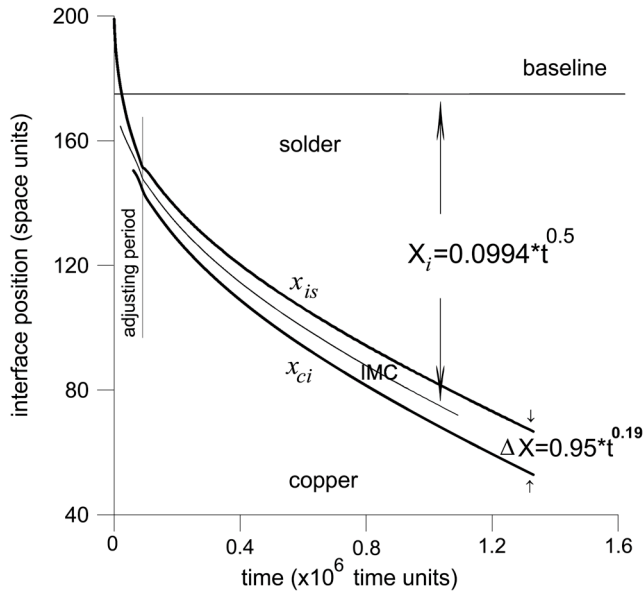
FIG. 5. Case B: Positions of the IMC/solder and IMC/copper boundaries vs time.

Fine[7] who showed that the thickening of IMC layer follows the temporal law for $\Delta X \propto t^{0.2}$, which is close to the numerical exponent of $n_{cs} = 0.19$. We do not exclude a possibility that this is a mere coincidence because the deviation from the parabolic law in the experiments can be caused by the factors which were not included in the present model, e.g., grain boundary diffusion.

The data on the average position of the layer in Fig. 5 fitted into the parabolic expression, $X_i = A_i t^{1/2}$, gave the numerical prefactor $A_i = 0.0994 \pm 0.001$, which matches closely the theoretical one, $B_i = 0.1055$, obtained from the CDM approximation of the three-phase Stefan problem, Eq. (A7), using the equilibrium solubilities from Table I. Overall, the numerical results present at least qualitative agreement with the experiments of Lord and Umantsev who showed that the IMC/solder and IMC/copper interfaces move in the direction of the copper, the creation-dissolution mechanism. Unfortunately the linear regime of CDM was not reproduced numerically because of the adjustment period, while the parabolic regime was not reproduced experimentally because the experiments were done on early stages only.

C. Case C: Limited amount of molten solder

In order to study the behavior of the system with limited amount of liquid solder we computed the model described by Eqs. (1)–(7) with different thicknesses of the solder phase: (a) 300, (b) 1300, and (c) 2500 space units. In this series of numerical experiments the simulations were not terminated when the concentration of Cu on the far end of the solder reached the level of 10^{-6}. In Fig. 6 are depicted positions of the boundaries of IMC layer versus time for three different initial thicknesses of the solder. Motion of the IMC/copper boundary is unidirectional towards the copper at all times of experiments. Motion of the IMC/solder boundary, however, is non-unidirectional: it starts moving in the direction of the copper phase but then stops, turns around, and starts moving

in the direction of the solder phase. If the simulations were continued long enough the molten solder and the solid copper phases would have been completely consumed by the growing IMC phase. These simulation results are in good qualitative agreement with the limited amount of solder experiments of Boettinger *et al.* (quantitative agreement is not possible here due to different compositions of the solder in the experiments and simulations).

In Fig. 6(d) is depicted the distribution of the concentration field for the initial amount of solder of 2500 space units at the time $t = 2.0 \times 10^6$, which is around the time of turnaround. Analysis of this concentration field clearly indicates that the turnaround occurs when solder reaches practically complete saturation.

IV. DISCUSSION

We introduced a continuum method for modeling of soldering reaction, which consists of dynamical equations, Eqs. (5)–(7), and the free energy expressions, Eqs. (1)–(3). We numerically simulated three common experimental situations relevant to the physical metallurgy of soldering: case A: IMC growth from an unlimited amount of solid-state solder (relatively low diffusion coefficient), case B: IMC growth from an unlimited amount of molten solder (relatively high diffusion coefficient), and case C: IMC growth from a limited amount of molten solder. We found qualitative agreement with experimental regimes of growth in all cases. For instance, the layer expands in both directions with respect to the base line at low temperatures and grows into the copper phase at high temperatures. In cases A and B the quantitative agreement with the sharp-interface approximation was also achieved. All this makes us believe that the continuum method may be used for quantitative modeling of an intermetallic phase growth from a molten solder. In addition, important physics of soldering has been learned: we found that in case C the turnaround of the IMC/solder boundary occurs approximately at the time of complete saturation of solder with copper. This result allows us to conclude that coarsening of IMC structure starts only after the solder is practically saturated with copper.

ACKNOWLEDGMENTS

APPENDIX A: THREE-PHASE STEFAN PROBLEM

In the framework of a three-phase Stefan problem, growth of an intermediate phase is described by the motion of two planar boundaries, which clamp the growing IMC layer. Mathematically, the problem is formulated for the concentration field, $c(x,t)$, which obeys diffusion equations in the bulk of each phase and two sets of boundary conditions, equilibrium and flux, at each boundary. For a more detailed description of a Stefan problem reader should consult the
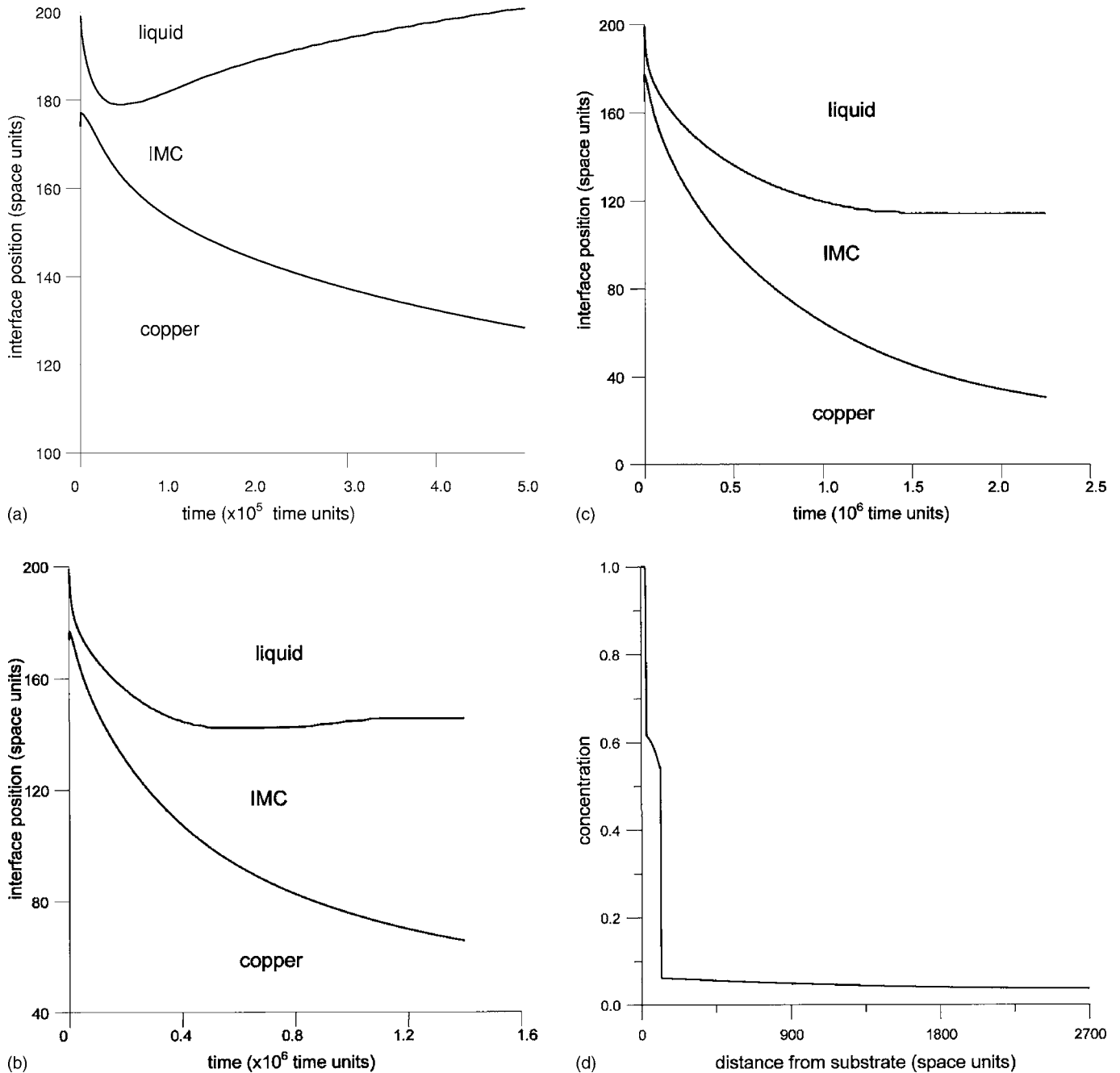
FIG. 6. Case C: Positions of the IMC/solder and IMC/copper boundaries vs time for different initial thicknesses of the solder: (a) 300, (b) 1300, and (c) 2500 space units. (d) Distribution of concentration in (c) at $t = 2.0 \times 10^6$.

literature.[11–13] The diffusion equations and boundary conditions may be easily derived as a sharp-interface limit from the continuum equations, Eqs. (5)–(7).[14–17]

The Stefan problem admits similarity solution, that is, motion of the boundaries with respect to their initial positions, the base line, is described by the square-root growth law. In this paper we take this law in the form

$$X_{\alpha i} = 2\beta_\alpha \sqrt{D_i t}, \quad \alpha = c, s, \tag{A1}$$

where the direction from the base line to the copper phase is chosen as positive. For the similarity solution (A1) to satisfy the boundary conditions, the growth-rate constants β_s and β_c must be determined from the following system of simulta-

neous transcendental equations [see Eqs. (7) and (8) in Ref. 12]:

$$\Delta C_i \frac{\exp(-\beta_c^2)}{\mathrm{erf}(\beta_c) - \mathrm{erf}(\beta_s)} - (1 - C_{c/i}) \frac{\exp(-\beta_c^2 (D_i/D_c))}{1 - \mathrm{erf}(\beta_c \sqrt{D_i/D_c})} \sqrt{\frac{D_c}{D_i}}$$
$$= \sqrt{\pi} \beta_c (C_{c/i} - C_{i/c}) \tag{A2a}$$

$$\Delta C_i \frac{\exp(-\beta_s^2)}{\mathrm{erf}(\beta_c) - \mathrm{erf}(\beta_s)} - (C_{s/i} - C_\infty) \frac{\exp(-\beta_s^2 (D_i/D_s))}{1 + \mathrm{erf}(\beta_s \sqrt{(D_i/D_s)})} \sqrt{\frac{D_s}{D_i}}$$
$$= -\sqrt{\pi} \beta_s (C_{i/s} - C_{s/i}) \tag{A2b}$$

Here C_∞ is the concentration in the solder far from the IMC layer, which does not change during the process, and ΔC_i

$\equiv (C_{i/c} - C_{i/s})$ is the interval of homogeneity of the intermediate phase.

Gibbs[12] analyzed the system of equations, Eqs. (A2), and found four limiting cases of solutions. One of them, the case of small growth rates (case D), is brought up here for purposes of comparison with the numerical results. Gibbs showed that if

$$\beta_s, \beta_c \ll \sqrt{\frac{D_c}{D_i}} \ll 1$$

and

$$\frac{\Delta C_i (C_{c/i} - C_{s/i} - \Delta C_i)}{(C_{c/i} - C_{i/c})(C_{s/i} - C_\infty)} \ll \frac{\sqrt{D_s D_c}}{D_i},$$

the system of equations, Eqs. (A2) may be resolved for $\Delta \beta \equiv \beta_c - \beta_s$,

$$\Delta \beta = \frac{\sqrt{\pi}}{2} \frac{\Delta C_i (C_{c/i} - C_{s/i} - \Delta C_i)}{(C_{c/i} - C_{i/c})(C_{s/i} - C_\infty)} \sqrt{\frac{D_i}{D_s}}, \qquad (A3)$$

which is proportional to the rate of IMC layer thickening.

Yet, there is another limiting case of solution of Eqs. (A2), important for comparison with the experimental and numerical simulation results presented in this paper, which was *not* analyzed in Ref. 12. This is the case when

$$1 \ll \beta_i \equiv \frac{1}{2}(\beta_s + \beta_c) \ll \sqrt{\frac{D_s}{D_i}},$$

$$\Delta \beta \ll \frac{1}{\beta_i}. \qquad (A4)$$

Here β_i is the average growth-rate constant of the intermediate phase. Using the properties of the error functions[21] one can find from Eqs. (A2) that

$$\beta_i (1 - C_{i/c}) = \frac{\Delta C_i}{2 \Delta \beta}, \qquad (A5a)$$

$$-\beta_i (C_{i/s} - C_{s/i}) = \frac{\Delta C_i}{2 \Delta \beta} - (C_{s/i} - C_\infty) \sqrt{\frac{D_s}{\pi D_i}}. \qquad (A5b)$$

Equations (A5) can be resolved for β_i and $\Delta \beta$ as follows:

$$\beta_i = \Theta \sqrt{\frac{D_s}{\pi D_i}}, \quad \Delta \beta = \frac{\Delta C_i}{2 \Theta (1 - C_{i/c})} \sqrt{\frac{\pi D_i}{D_s}},$$

$$\Theta \equiv \frac{C_{s/i} - C_\infty}{1 - C_{s/i} - \Delta C_i}. \qquad (A6)$$

Here Θ is the undersaturation of the solder. Both interfaces in this case move in the same direction—towards the copper phase—with nearly equal, but still slightly different velocities, which allows for the intermediate phase thickening. Thus, this case describes the CDM of Lord and Umantsev. For the average position of the layer Eqs. (A1), (A4), and (A6) yield

$$X_i \equiv 2 \beta_i \sqrt{D_i t} = \frac{2}{\sqrt{\pi}} \Theta \sqrt{D_s t}. \qquad (A7)$$

The CDM approximation works if the diffusion in the solder is much faster than in the intermediate and copper phases, $D_s \gg D_i, D_c$, the interval of homogeneity of the intermediate phase is very narrow, $\Delta C_i \ll 1$, and the solubility limit in the solder is very small, $C_{s/i} \ll 1$. These thermodynamic and kinetic conditions are met in the Cu–Sn solid-liquid diffusion couple. Notice, however, that CDM does not work for the case of a saturated solder, $\Theta = 0$.

APPENDIX B: EQUILIBRIUM PHASE DIAGRAM IN BINARY PARABOLIC SYSTEM

We define a parabolic thermodynamic system as a substance where the molar Gibbs free energy as a function of concentrations of its components is described by a polynomial of the second order. We consider here the conditions of equilibrium coexistence of two phases, α and β, both of which are parabolic systems. Additional simplification here comes from the fact that both phases are formed only by two species, so that their compositions may be described by the mole fraction of the solute, c. Then, the coexistence of a binary parabolic system is described by the molar free energies of phases in the forms

$$G_\alpha = G_{\alpha,0} + G_{\alpha,1} c + \frac{1}{2} G_{\alpha,2} c^2, \quad G_{\alpha,2} > 0,$$

$$G_\beta = G_{\beta,0} + G_{\beta,1} c + \frac{1}{2} G_{\beta,2} c^2, \quad G_{\beta,2} > 0. \qquad (B1)$$

The phase diagram of such system consists of the concentrations of the phases, $C_{\alpha/\beta}$ and $C_{\beta/\alpha}$, that coexist at equilibrium with each other. The conditions $0 < C_{\alpha/\beta}, C_{\beta/\alpha} < 1$ must be imposed separately because the parabolic free energy does not have singularities at the points $c = 0$ or 1.

Mathematically, coexistence of the phases can be expressed by the condition of common tangency,[22] that is that the straight line $y = kc + l$ is the tangent to both curves in Eqs. (B1) simultaneously. Then we obtain a system of four simultaneous equations for four unknowns,

$$G_{\alpha,0} + G_{\alpha,1} C_{\alpha/\beta} + \frac{1}{2} G_{\alpha,2} C_{\alpha/\beta}^2 = l + k C_{\alpha/\beta},$$

$$G_{\alpha,1} + G_{\alpha,2} C_{\alpha/\beta} = k,$$

$$G_{\beta,0} + G_{\beta,1} C_{\beta/\alpha} + \frac{1}{2} G_{\beta,2} C_{\beta/\alpha}^2 = l + k C_{\beta/\alpha},$$

$$G_{\beta,1} + G_{\beta,2} C_{\beta/\alpha} = k. \qquad (B2)$$

Simple algebraic manipulations transform this system into two equations for equilibrium concentrations only,

$$[G_2] C_{\alpha/\beta}^2 + 2[G_1] C_{\alpha/\beta} - \frac{[G_1]^2}{G_{\alpha,2}} + 2 \frac{G_{\beta,2}}{G_{\alpha,2}} [G_0] = 0, \qquad (B3a)$$

$$C_{\beta/\alpha} = \frac{G_{\alpha,2} C_{\alpha/\beta} - [G_1]}{G_{\beta,2}}, \tag{B3b}$$

where $[G] \equiv G_\beta - G_\alpha$. For $C_{\alpha/\beta}$ and $C_{\beta/\alpha}$ to exist the discriminant $\mathbb{D}$ must be positive,

$$\mathcal{D} \equiv [G_1]^2 - 2[G_0][G_2] > 0. \tag{B4}$$

If $[G_2] \neq 0$, Eqs. (B3) can be resolved as follows:

$$C_{\alpha/\beta}^{\pm} = \frac{-[G_1] \pm \sqrt{(G_{\beta,2}/G_{\alpha,2})\mathcal{D}}}{[G_2]}, \tag{B5}$$

$$C_{\beta/\alpha}^{\pm} = \frac{-[G_1] \pm \sqrt{(G_{\alpha,2}/G_{\beta,2})\mathcal{D}}}{[G_2]}.$$

A particular simple case of a parabolic system with $[G_2]=0$ was previously studied in Refs. 16 and 17 It was named linear because of the disappearance of the quadratic term in the equations for the equilibrium concentrations, see Eq. (B3a). Physically the linear system describes many cases of crystallization/melting transition in isomorphous systems. In this case,

$$C_{\alpha/\beta} = \frac{[G_1]}{2G_2} - \frac{[G_0]}{[G_1]}, \quad C_{\beta/\alpha} = -\frac{[G_1]}{2G_2} - \frac{[G_0]}{[G_1]}. \tag{B6}$$

[1] C. Lea, *A Scientific Guide to Surface Mount Technology* (Electrochemical, Ayr, 1988), p. 309.

[2] J. D. Bernal, Nature (London) **122**, 54 (1928).

[3] A. Gangulee, G. C. Das, and M. B. Bever, Metall. Trans. **4**, 2063 (1973).

[4] M. Onishi and H. Fujibuchi, Trans. Jpn. Inst. Met. **16**, 539 (1975).

[5] A. Hayashi, C. R. Kao, and Y. A. Chang, Scr. Mater. **37**, 393 (1997).

[6] H. K. Kim, H. K. Liou, and K. N. Tu, Appl. Phys. Lett. **66**, 2337 (1995).

[7] R. A. Gagliano and M. E. Fine, J. Electron. Mater. **32**, 1441 (2003).

[8] H. K. Kim and K. N. Tu, Phys. Rev. B **53**, 1 (1996).

[9] W. J. Boettinger, K.-W. Moon, and C. A. Handwerker, Fall ASM/TMS Meeting, Cincinnati, OH, 1 November, 1999 (unpublished).

[10] R. A. Lord and A. Umantsev, J. Appl. Phys., **98**, 063525 (2005).

[11] J. S. Kirkaldy, Can. J. Phys. **36**, 917 (1958); W. Jost, *Diffusion in Solids, Liquids, Gases* (Academic, New York, NY, 1952), pp. 68–75; W. Seith and T. Heumann, *Diffusion of Metals: Exchange Reactions* (Springer, Berlin, 1955), pp. 150–154; C. Wagner, Acta Metall. **17**, 99 (1969) ; L. I. Rubinstein, *The Stefan Problem* (American Mathematical Society, Providence, RI, 1971), pp. 141–189; B. Ya. Lyubov, *Kinetic Theory of Phase Transformations* (National Bureau of Standards, Gaithersburg, MD, 1978), pp. 88–94.

[12] G. B. Gibbs, J. Nucl. Mater. **20**, 303 (1966).

[13] Z. Mei, A. J. Sunwoo, and J. W. Morris, Jr., Metall. Trans. A **23A**, 857 (1992).

[14] N. A. Ahmad, A. A. Wheeler, W. J. Boettinger, and G. B. McFadden, Phys. Rev. E **58**, 3436 (1998).

[15] A. Karma, Phys. Rev. Lett. **87**, 115701 (2001).

[16] A. Umantsev, Phys. Rev. B **64**, 075419 (2001); Phys. Rev. E **69**, 016111 (2004).

[17] A. Umantsev, Phys. Rev. B **74**, 22 (2006).

[18] Data from Thermocalc© database were provided by G. Ghosh.

[19] R. L. J. M. Ubachs, P. J. G. Schreurs, and M. G. D. Geers, Int. J. Solids Struct. **42**, 2533 (2005); W. Dreyer and W. Muller, *ibid.* **37**, 3841 (2000).

[20] R. J. Ravelo and M. I. Baskes, Mater. Res. Soc. Symp. Proc. **398**, 287–293 (1996).

[21] M. Abramowitz and I. Stegun, *Handbook of Mathematical Functions* (National Bureau of Standards, Gaithersburg, MO, 1964).

[22] C. H. P. Lupis, *Chemical Thermodynamics of Materials* (North-Holland, New York, 1983), p. 67.